



HAL
open science

Mg₃(BH₄)₄(NH₂)₂ as Inorganic Solid Electrolyte with High Mg²⁺ Ionic Conductivity

Ronan Le Ruyet, Benoit Fleutot, Romain Berthelot, Yasmine Benabed, Geoffroy Hautier, Yaroslav Filinchuk, Raphael Janot

► To cite this version:

Ronan Le Ruyet, Benoit Fleutot, Romain Berthelot, Yasmine Benabed, Geoffroy Hautier, et al.. Mg₃(BH₄)₄(NH₂)₂ as Inorganic Solid Electrolyte with High Mg²⁺ Ionic Conductivity. ACS Applied Energy Materials, ACS, 2020, 3 (7), pp.6093-6097. 10.1021/acsaem.0c00980 . hal-02924388

HAL Id: hal-02924388

<https://hal.umontpellier.fr/hal-02924388>

Submitted on 1 Dec 2020

HAL is a multi-disciplinary open access archive for the deposit and dissemination of scientific research documents, whether they are published or not. The documents may come from teaching and research institutions in France or abroad, or from public or private research centers.

L'archive ouverte pluridisciplinaire **HAL**, est destinée au dépôt et à la diffusion de documents scientifiques de niveau recherche, publiés ou non, émanant des établissements d'enseignement et de recherche français ou étrangers, des laboratoires publics ou privés.

Mg₃(BH₄)₄(NH₂)₂ as Inorganic Solid Electrolyte with High Mg²⁺ Ionic Conductivity

Ronan Le Ruyet,^{a,d} Benoît Fleutot,^{a,d} Romain Berthelot,^{b,d} Yasmine Benabed,^{c,e} Geoffroy Hautier,^c Yaroslav Filinchuk,^c and Raphaël Janot^{a,d,*}

^a *Laboratoire de Réactivité et Chimie des Solides (LRCS), Université de Picardie Jules Verne, UMR 7314 CNRS, 33 Rue Saint Leu, Amiens 80039, France.*

^b *ICGM, Univ. Montpellier, UMR 5253 CNRS, ENSCM, Montpellier, France.*

^c *Institute of Condensed Matter and Nanosciences, Université catholique de Louvain, Place L. Pasteur 1, Louvain-la-Neuve 1348, Belgium.*

^d *Réseau sur le Stockage Electrochimique de l'Energie (RS2E), FR 3459 CNRS, 33 Rue Saint Leu, Amiens 80039, France.*

^e *Department of Chemistry, Université de Montréal, Montreal, H3T1J4, Canada.*

* Corresponding author: Raphaël Janot: raphael.janot@u-picardie.fr

Co-authors: Ronan Le Ruyet: ronan.leruyet@u-picardie.fr

Benoît Fleutot: benoit.fleutot@u-picardie.fr

Romain Berthelot: romain.berthelot@umontpellier.fr

Yasmine Benabed: y.benabed@hotmail.fr

Geoffroy Hautier: geoffroy.hautier@uclouvain.be

Yaroslav Filinchuk: yaroslav.filinchuk@uclouvain.be

Abstract

$\text{Mg}_3(\text{BH}_4)_4(\text{NH}_2)_2$ compound was synthesized through the investigation of the $\text{Mg}(\text{BH}_4)_2$ - $\text{Mg}(\text{NH}_2)_2$ phase diagram; its crystal structure was solved in a tetragonal unit cell with the space group I-4. Interestingly, $\text{Mg}_3(\text{BH}_4)_4(\text{NH}_2)_2$ has a high thermal stability with a decomposition temperature above 190°C and exhibits a high Mg^{2+} ionic conductivity of $4.1 \times 10^{-5} \text{ S}\cdot\text{cm}^{-1}$ at 100°C with a low activation energy (0.84 eV). The reversible Mg deposition/stripping was demonstrated at 100°C when using $\text{Mg}_3(\text{BH}_4)_4(\text{NH}_2)_2$ as solid electrolyte. Thus, $\text{Mg}_3(\text{BH}_4)_4(\text{NH}_2)_2$ is a compound that could help to develop rechargeable Mg-ion solid-state batteries.

Keywords: ionic conductor, Mg-ion battery, borohydride, crystal structure, impedance spectroscopy

In order to develop rechargeable batteries with better energy density and more sustainable materials than the lithium-based batteries, post-Li-ion technologies are being developed.¹ Among them, magnesium-based batteries are studied as Mg has the advantages of being abundant in the earth crust (21100 ppm vs. 10 ppm for Li),² to have a low redox potential (-2.356 V vs. NHE) and a high volumetric capacity ($3833 \text{ mAh}\cdot\text{cm}^{-3}$ vs. $2046 \text{ mAh}\cdot\text{cm}^{-3}$ for Li). Nevertheless, the development of Mg batteries is slowed down by the difficulty of finding proper electrolytes. Until now, most of the liquid electrolytes used in Mg-ion batteries were made on Cl-containing salts (e.g. Grignard reagents), which cause severe corrosions to the electrochemical cell if the working potential is too high.^{3,4} Recent progress has been made with fluoro-alkoxy-borates salts, such as $\text{Mg}(\text{B}(\text{hfip})_4)_2$ with $\text{hfip} = \text{OCH}(\text{CF}_3)_2$, which are chlorine-free and show high electrochemical stability up to 4.5 V (vs. Mg^{2+}/Mg).⁵ Interestingly,

hydroborate and carbo-borate based compounds (e.g. $\text{Mg}(\text{BH}_4)_2$ and $\text{Mg}(\text{CB}_{11}\text{H}_{12})_2$) were also recently investigated as Mg^{2+} salts.⁶ These liquid electrolytes remain however limited for high energy density devices due to reactions occurring at the electrolyte/positive electrode interface. In addition, all these liquid electrolytes suffer from the use of ether-based solvents (often THF or DME) which are very volatile and flammable. Finally, quite recently, it has been demonstrated that the long thought non-dendritic formation in the case of Mg-ion batteries is false: several groups have reported that Mg dendritic growth can also occur and lead to fatal failures.⁷⁻⁸

As for Li-ion and Na-ion batteries, there is an increasing interest for all-solid-state batteries in the case of Mg-ion as it could definitively solve the issues of solvent leakage and flammability. In addition, it could possibly allow the use of Mg metal at the negative electrode without any magnesium dendritic formation if the solid electrolyte pellet is dense enough. Thus, inorganic solid electrolytes could largely improve rechargeable Mg batteries if their ionic conductivity and electrochemical stability window are high. Unfortunately, inorganic solid compounds with Mg^{2+} cations have very low ionic conductivities, due to the very sluggish diffusion of divalent Mg^{2+} in the solid. Two recent reviews give a nice picture of the family of materials exhibiting decent Mg^{2+} ionic conductivities.^{9,10} Among them, the NASICON-like phosphates (e.g. $\text{MgZr}_4(\text{PO}_4)_6$) show a high ionic conductivity of about $10^{-3} \text{ S.cm}^{-1}$, however at high temperature (800°C),¹¹ and thus are unsuitable for Mg^{2+} rechargeable batteries. Searching for compounds with higher conductivities, and similarly to what is known for lithium, oxygen can be replaced by sulfur in Mg^{2+} ionic solid conductors. Indeed, sulfide glasses and glass-ceramics (e.g. $\text{MgS-P}_2\text{S}_5$) show an improved Mg^{2+} cation mobility at lower temperatures, but the ionic conductivity is still too low for applications (around $10^{-8} \text{ S.cm}^{-1}$ at 200°C).¹² A recent class of materials with high ionic conductivities are the ternary spinels,¹³ such as MgSc_2Se_4 ($10^{-4} \text{ S.cm}^{-1}$ at 25°C), but unfortunately, these conductivities are accompanied by high electronic

ones (about $4 \times 10^{-8} \text{ S.cm}^{-1}$), which impede their possible use as solid electrolytes.¹⁴ As a matter of fact, similarly to the recently developed Mg^{2+} salts based on $\text{Mg}(\text{BH}_4)_2$ for liquid electrolytes, the most interesting materials for solid electrolytes are today based on the same compound and derivatives.¹⁵ Very recent studies have shown the possibility to reach high ionic conductivities of about $10^{-5} \text{ S.cm}^{-1}$ close to room temperature by adding neutral molecules to $\text{Mg}(\text{BH}_4)_2$. In this manner, $\text{Mg}(\text{en})_1(\text{BH}_4)_2$ with *en* being ethylene-diamine, $\text{Mg}(\text{BH}_4)_2\text{-NH}_3$ and $\text{Mg}(\text{BH}_4)_2(\text{NH}_3\text{BH}_3)_2$ reach ionic conductivities of $6 \times 10^{-5} \text{ S.cm}^{-1}$ at 70°C ,¹⁶ $8.5 \times 10^{-5} \text{ S.cm}^{-1}$ at 70°C ,¹⁷ and $8.4 \times 10^{-5} \text{ S.cm}^{-1}$ at 40°C ,¹⁸ respectively. The latter is indeed the solid compound with the highest Mg^{2+} ionic conductivity reported so far. The ionic conductivity enhancement when adding these neutral N-H containing molecules is attributed to a network of dihydrogen $\text{N-H}^{\delta+} \dots \delta\text{-H-B}$ bonds allowing a high degree of structural flexibility, as already observed in the field of hydrogen storage materials,¹⁹ and to the large volume of the tetrahedra surrounding the Mg^{2+} cations allowing a facilitated Mg^{2+} ionic motion.

In the literature, $\text{Mg}(\text{BH}_4)(\text{NH}_2)$ compound was reported to have an ionic conductivity of $1 \times 10^{-6} \text{ S.cm}^{-1}$ at 150°C ,²⁰ but we have recently demonstrated that this conductivity could be improved up to $3 \times 10^{-6} \text{ S.cm}^{-1}$ at only 100°C by synthesizing a glass-ceramic-like material.²¹ This was due to the presence of an unknown additional amorphous compound that was assumed as another phase existing in the $\text{Mg}(\text{BH}_4)_2\text{-Mg}(\text{NH}_2)_2$ binary system. Indeed, in similar systems such as $\text{LiBH}_4\text{-LiNH}_2$, several compounds can be obtained for different compositions.²² Searching for other magnesium ionic conductors, we explored different compositions in the hitherto unknown $\text{Mg}(\text{BH}_4)_2\text{-Mg}(\text{NH}_2)_2$ binary phase diagram (cf. Figure S1) by ball-milling and annealing of various mixtures of $\text{Mg}(\text{BH}_4)_2$ and $\text{Mg}(\text{NH}_2)_2$.

After ball-milling and annealing at 120°C of a $\text{Mg}(\text{BH}_4)_2\text{:Mg}(\text{NH}_2)_2$ mixture in the 2:1 molar ratio (see the supporting information for the detailed synthesis conditions), a crystalline single-phase compound was obtained and, consequently, named $\text{Mg}_3(\text{BH}_4)_4(\text{NH}_2)_2$ (cf. Figure

S1 for the experimentally determined $\text{Mg}(\text{BH}_4)_2\text{-Mg}(\text{NH}_2)_2$ binary phase diagram). The corresponding XRD pattern has been well indexed in a tetragonal unit cell (cf. Figure 1a) like other compounds in the $\text{Mg}(\text{BH}_4)_2\text{-Mg}(\text{NH}_2)_2$ phase diagram, for instance: $\text{Mg}(\text{BH}_4)(\text{NH}_2)$ (space group: $I4_1$),²³ $\text{Mg}(\text{NH}_2)_2$ (space group: $I4_1/\text{acd}$)²⁴ and $\delta\text{-Mg}(\text{BH}_4)_2$ (space group: $I4_1/\text{acd}$)²⁵. From Rietveld refinement with the space group I-4, it was possible to propose a crystal structure for the so-called $\text{Mg}_3(\text{BH}_4)_4(\text{NH}_2)_2$ with tetragonal cell parameters $a = 14.1801(8) \text{ \AA}$ and $c = 6.002(4) \text{ \AA}$ (cf. Figure 1b). Only few additional weak peaks of $\text{Mg}(\text{BH}_4)(\text{NH}_2)$ can be observed (i.e. a content of only 1.1 wt.% as found from Rietveld refinement).

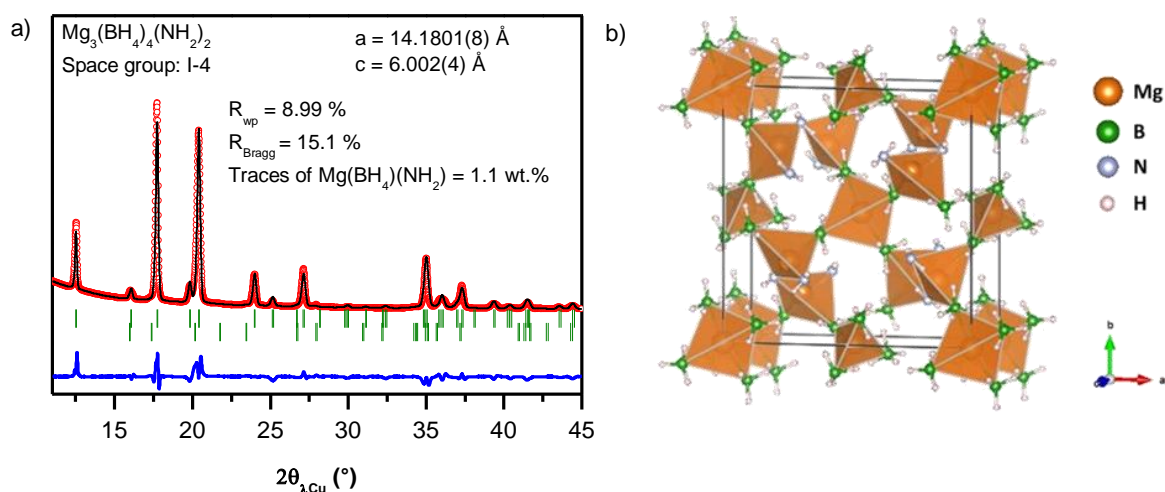


Figure 1. a) Rietveld refinement of the XRD diagram of $\text{Mg}_3(\text{BH}_4)_4(\text{NH}_2)_2$ and b) its crystal structure drawn with the software VESTA.

Crystal structure of $\text{Mg}_3(\text{BH}_4)_4(\text{NH}_2)_2$, solved in the space group I-4, is shown in Figure 1b. The presence of some weak peaks allowed to exclude the screw axis 4_1 and the glide planes. Twelve Mg atoms per cell are distributed over three crystallographic sites, the anions were also attributed to three sites: 8 + 8 for BH_4 groups and one 8-fold position for NH_2 (cf. Table S1). The site for the NH_2 group is clearly identified thanks to much shorter Mg-N bonds than Mg...B

contacts, as well as by much narrower N-Mg-N angles compared to rather open B...Mg...B, as also seen in the crystal structures of Mg(NH₂)₂ and Mg(BH₄)₂. A possible anionic site disorder cannot be firmly excluded due to the small difference in the X-ray scattering power for the BH₄ and NH₂ anions, however it not supported the distinctly different structural chemistry of the anions. The B-H distance of 1.15 Å and N-H of 0.9 Å were taken as typical values for the apparent bond lengths for X-ray diffraction studies, the H-B-H and H-N-H angles were fixed as ideally tetrahedral (109.47°). The positions and the orientations of the anions, determined using the software FOX with the help of H...H anti-bump restraints, were fixed in the latter refinement. The experimental structure was DFT-optimized, improving accuracy of hydrogen positions (the major difference with the experimental structure is related to the anions' orientations) and validating the experimental conclusions. The full crystallographic parameters can be found in Table S1. Two Mg sites (Mg1 and Mg2) are in the center of tetrahedra made of four (BH₄)⁻ anions as in Mg(BH₄)₂ and one site (Mg3) is in the center of a tetrahedron made of two (BH₄)⁻ anions and two (NH₂)⁻ anions as in Mg(BH₄)(NH₂). The calculated density for Mg₃(BH₄)₄(NH₂)₂ crystal structure is very low: 0.904 g.cm⁻³. This low crystallographic density is attractive for a solid-state electrolyte as it allows obtaining good ionic percolation in composite electrodes with a relatively low weight of electrolyte, thus ensuring reasonable electrochemical gravimetric capacities for the composite electrodes.

Infrared spectroscopy was performed on this Mg₃(BH₄)₄(NH₂)₂ compound (cf. Figure S2) and reveals N-H and B-H stretching/bending bands at very similar wave numbers to those found for the precursors, Mg(BH₄)₂ and Mg(NH₂)₂, and to the other compound in the binary diagram: Mg(BH₄)(NH₂). More specifically, two strong N-H stretching bands are observed at 3270 and 3326 cm⁻¹ which are characteristic values of (NH₂)⁻ anion close to Mg²⁺ and it must be noticed that no band is visible around 3150-3200 cm⁻¹, thus confirming the absence of imide (NH)²⁻ moieties. Interestingly, in the 1000-1600 cm⁻¹ range, it can be observed that the B-H bending

bands are split into two compared to the spectrum of $\text{Mg}(\text{BH}_4)(\text{NH}_2)$, which agrees well with the XRD refinement showing two different Wyckoff positions for the B atoms (vs. only one position in the case of $\text{Mg}(\text{BH}_4)(\text{NH}_2)$).

The thermal stability of $\text{Mg}_3(\text{BH}_4)_4(\text{NH}_2)_2$ was evaluated by Thermogravimetric Analysis (TGA) coupled with Differential Thermal Analysis (DTA) measurements (cf. Figure S3). Very importantly, no mass loss or exo/endermic phenomenon was observed up to 190°C under argon. Only a slight decrease of the mass (less than 0.1 %) can be observed starting around 190°C , which is probably related to the beginning of the compound decomposition. Above 200°C , the compound readily decomposes forming a foamy material due to gas releases (a mixture of H_2 and NH_3). Nevertheless, the fact that $\text{Mg}_3(\text{BH}_4)_4(\text{NH}_2)_2$ remains stable at temperatures up to 190°C is very interesting, especially when compared to the recently reported compounds obtained by the addition of a neutral molecule to $\text{Mg}(\text{BH}_4)_2$ (molecules such as *en* = $\text{C}_2\text{H}_4(\text{NH}_2)_2$, NH_3 , or NH_3BH_3). These compounds are indeed clearly less thermally stable than $\text{Mg}_3(\text{BH}_4)_4(\text{NH}_2)_2$: $\text{Mg}(\text{en})_1(\text{BH}_4)_2$ has a phase transition at 75°C and starts to be decomposed at 100°C , $\text{Mg}(\text{BH}_4)_2\text{-NH}_3$ is decomposed at 138°C ,²⁶ whereas $\text{Mg}(\text{BH}_4)_2(\text{NH}_3\text{BH}_3)_2$ melts at 48°C and starts to be decomposed at 85°C .²⁷ Even, $\text{Mg}(\text{BH}_4)(\text{NH}_2)$, the only other compound reported in the $\text{Mg}(\text{BH}_4)_2\text{-Mg}(\text{NH}_2)_2$ phase diagram, becomes amorphous around 150°C and starts to be decomposed at 200°C (cf. Figure S1).

Owing to the good thermal stability of $\text{Mg}_3(\text{BH}_4)_4(\text{NH}_2)_2$, its ionic conductivity was measured on pellets by Electrochemical Impedance Spectroscopy (EIS) as a function of temperature. All Nyquist plots show the same shape as the one recorded at 100°C (cf. Figure 2a) *i.e.* only one semicircle at high frequency, that is attributed to the ionic conduction in the material, followed by a straight line at low frequency, that is the capacitance caused by the ion blocking electrodes placed on both sides of the pelletized sample. The ionic conductivity increases from $6.2 \times 10^{-7} \text{ S.cm}^{-1}$ at 50°C to $4.1 \times 10^{-5} \text{ S.cm}^{-1}$ at 100°C (cf. Figure 2b). These values

are among the highest recorded for a purely inorganic Mg^{2+} solid ionic conductor at such low temperatures. We can notice that the conductivity values remain exactly the same upon cooling (and upon the subsequent heating/cooling cycles not shown here) confirming that the sample does not undergo any thermal degradation. Actually, the impedance spectroscopy measurements were performed up to 100°C , a much lower temperature than the degradation temperature of above 190°C previously determined by TGA/DTA.

It is interesting to compare the high conductivity of $4.1 \times 10^{-5} \text{ S.cm}^{-1}$ at 100°C with the one of $3 \times 10^{-6} \text{ S.cm}^{-1}$ that we have previously obtained at the same temperature for a $\text{Mg}(\text{BH}_4)(\text{NH}_2)$ glass-ceramic material. $\text{Mg}_3(\text{BH}_4)_4(\text{NH}_2)_2$ compound has undoubtedly an improved ionic conductivity and a higher thermal stability. The activation energy for the ionic conduction of $\text{Mg}_3(\text{BH}_4)_4(\text{NH}_2)_2$ was found to be 0.84 eV from the plot of $\ln(\sigma.T)$ as a function of $1/T$. This activation energy is low, indicating a high mobility of the Mg^{2+} cations. Indeed, E_a extracted from the plot of $\ln(\sigma.T)$ as a function of $1/T$ is the addition of the energy needed to form the mobile charge carrier (E_f) and the energy barrier for its migration (E_m).²⁸ If E_a is low, then the Mg^{2+} cations are easily formed and/or have a favourable path and low energy barrier to migrate. In both cases, the low activation energy (0.84 eV) means a better mobility of the Mg^{2+} cations compared to similar compounds with higher activation energies.

The lowest activation energies reported in inorganic solid Mg^{2+} electrolytes were 0.83 - 0.88 eV in $\text{MgZr}_4(\text{PO}_4)_6$ and related materials.^{29,30} The activation energy of $\text{Mg}_3(\text{BH}_4)_4(\text{NH}_2)_2$ is also much lower than the ones measured for other $\text{Mg}(\text{BH}_4)_2$ -based solid electrolytes: 1.2 , 1.47 , 1.6 , and 2.0 eV for $\text{Mg}(\text{BH}_4)(\text{NH}_2)$, $\text{Mg}(\text{BH}_4)_2(\text{NH}_3\text{BH}_3)_2$, $\text{Mg}(\text{en})_1(\text{BH}_4)_2$, and $\text{Mg}(\text{BH}_4)_2\text{-NH}_3$, respectively. The good mobility of Mg^{2+} in $\text{Mg}_3(\text{BH}_4)_4(\text{NH}_2)_2$ is not fully understood yet but it might be linked to its unique crystal structure in which Mg^{2+} cations occupied mixed sites between tetrahedra made of four $(\text{BH}_4)^-$ anions and others made of two $(\text{BH}_4)^-$ anions and two $(\text{NH}_2)^-$ anions, and the role of the dihydrogen bonds (of 2.11 and 2.23 \AA

in the DFT-optimized structure). Deeper structural characterizations, if possible on single crystals, could be also useful to check the possible formation of vacancies, especially on the N crystallographic sites, which could promote largely the Mg^{2+} mobility.

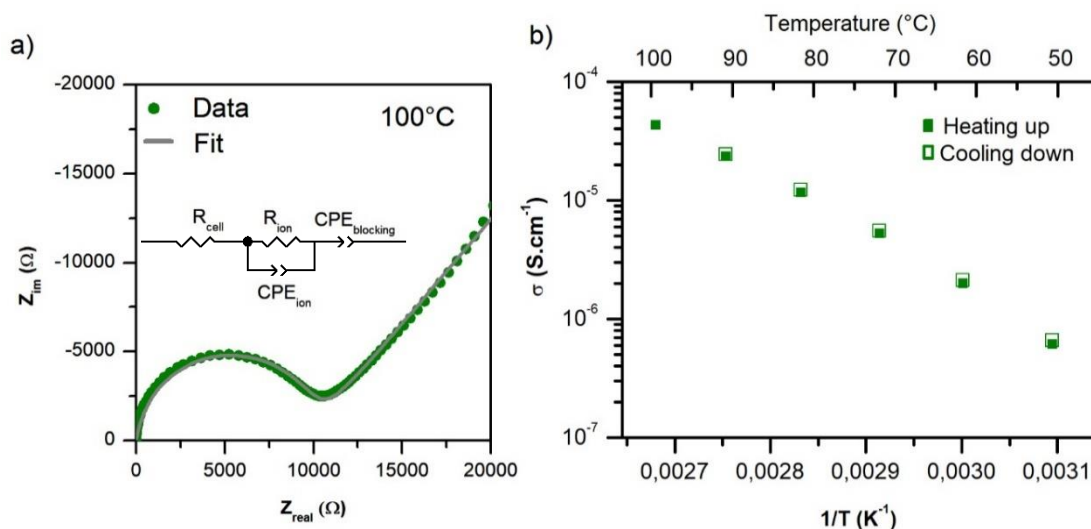


Figure 2. a) Nyquist plot obtained by EIS at 100°C for $\text{Mg}_3(\text{BH}_4)_4(\text{NH}_2)_2$ and b) the ionic conductivity as a function of $1/T$.

As $\text{Mg}_3(\text{BH}_4)_4(\text{NH}_2)_2$ is among the compound with the highest Mg^{2+} ionic conductivity, it was important to prove that reversible Mg deposition/stripping is possible and that its use as electrolyte in all solid-state Mg-ion batteries could be realized. In order to determine the Electrochemical Stability Window (ESW), cyclic voltammetry measurements were done at 100°C on a composite working electrode (WE) made by mixing $\text{Mg}_3(\text{BH}_4)_4(\text{NH}_2)_2$ with 10 wt.% of carbon black, the latter needed to bring electrons in the material and, thus, to really evaluate its electrochemical stability. This composite WE was separated from the Mg counter electrode by a layer of pure $\text{Mg}_3(\text{BH}_4)_4(\text{NH}_2)_2$.

When starting the cyclic voltammetry with a sweep towards low potentials first, a strong reduction peak assigned to Mg deposition is clearly visible below 0 V vs. Mg^{2+}/Mg (cf. Figure 3). This phenomenon is partially reversible as the corresponding Mg stripping occurs

upon oxidation. The coulombic efficiency at this first cycle is about 20 %, which might be improved by a better mixing of the carbon with the solid electrolyte (here simply made with an agate mortar). No reduction peak other than the Mg deposition occurred so the $\text{Mg}_3(\text{BH}_4)_4(\text{NH}_2)_2$ solid electrolyte is stable at low potentials. This result is interesting because solid electrolytes often react with a metallic anode. On the other side, the oxidation of the $\text{Mg}_3(\text{BH}_4)_4(\text{NH}_2)_2$ solid electrolyte is unfortunately observed with an onset potential of about 1.48 V vs Mg^{2+}/Mg . This oxidation is irreversible and the exact reaction occurring is not fully identified, but it is most probably related to the oxidation of the $(\text{NH}_2)^-$ moieties. It is noteworthy that the coulombic efficiency of the Mg deposition/stripping remains around 20 % for the first 5 cycles meaning that the decomposition products formed upon oxidation do not affect this process. The ESW of $\text{Mg}_3(\text{BH}_4)_4(\text{NH}_2)_2$ ranges from 0 to 1.48 V vs. Mg^{2+}/Mg which is similar to the ESWs previously reported for $\text{Mg}(\text{en})_1(\text{BH}_4)_2$ and $\text{Mg}(\text{BH}_4)_2(\text{NH}_3\text{BH}_3)_2$ (i.e. 0 to 1.2 V vs. Mg^{2+}/Mg for both of them).

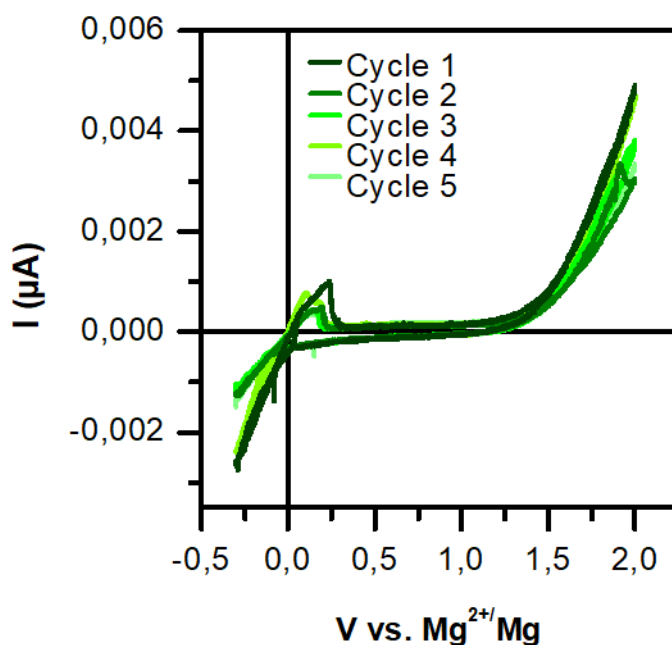


Figure 3. Cyclic voltammetry measurement at 100°C and 0.05 $\text{mV}\cdot\text{s}^{-1}$ of a cell made of $\text{Mg} / \text{Mg}_3(\text{BH}_4)_4(\text{NH}_2)_2 / \text{Mg}_3(\text{BH}_4)_4(\text{NH}_2)_2 + \text{carbon (90:10 wt.\%)}$.

In conclusion, a compound with the $\text{Mg}_3(\text{BH}_4)_4(\text{NH}_2)_2$ stoichiometry was synthesized when exploring the $\text{Mg}(\text{BH}_4)_2$ - $\text{Mg}(\text{NH}_2)_2$ binary phase diagram. The crystal structure of $\text{Mg}_3(\text{BH}_4)_4(\text{NH}_2)_2$ was solved in a tetragonal unit cell with the I-4 space group, where the Mg^{2+} cations occupy three different Wyckoff sites in distorted tetrahedra. Interestingly, the $\text{Mg}_3(\text{BH}_4)_4(\text{NH}_2)_2$ compound has a thermal stability up to 190°C , which is higher than those of the compounds recently reported, based on addition of neutral molecules to $\text{Mg}(\text{BH}_4)_2$. The ionic conductivity of $\text{Mg}_3(\text{BH}_4)_4(\text{NH}_2)_2$ is among the highest ever measured at low temperatures for a purely inorganic Mg^{2+} ionic conductor with a value of $4.1 \times 10^{-5} \text{ S}\cdot\text{cm}^{-1}$ at 100°C and a low activation energy (0.84 eV). Its electrochemical stability window was determined as ranging from 0 to 1.48 V vs. Mg^{2+}/Mg , which are common voltages for $\text{Mg}(\text{BH}_4^-)$ - (NH_x) based solid electrolytes. The reversible Mg deposition/stripping was demonstrated at 100°C and $\text{Mg}_3(\text{BH}_4)_4(\text{NH}_2)_2$ is indeed a very interesting Mg^{2+} ionic conductor that could help to develop better rechargeable Mg-ion batteries.

Acknowledgements

The RS2E (French network on electrochemical energy storage) is acknowledged for the PhD funding of Ronan Le Ruyet (STORE-EX Labex Project ANR-10-LABX-76-01) and the Communauté Française de Belgique for the support under grant ARC 18/23-093. Matthieu Courty (LRCS, UPJV, Amiens) is also thanked for the thermal analysis measurements. The present research benefited from computational resources made available on the Tier-1 supercomputer of the Fédération Wallonie-Bruxelles, infrastructure funded by the Walloon Region under grant agreement n°1117545.

Supporting Information Available

Experimental section including conditions for material synthesis, characterizations and electrochemical measurements; Table listing the parameters for the experimentally solved and the DFT-optimized structures of the new $\text{Mg}_3(\text{BH}_4)_4(\text{NH}_2)_2$ compound; computational methods. Figures showing the experimentally determined $\text{Mg}(\text{BH}_4)_2$ - $\text{Mg}(\text{NH}_2)_2$ binary phase diagram, the infrared spectra of $\text{Mg}(\text{BH}_4)_2$, $\text{Mg}(\text{NH}_2)_2$, $\text{Mg}(\text{BH}_4)(\text{NH}_2)$ and $\text{Mg}_3(\text{BH}_4)_4(\text{NH}_2)_2$ and, the thermal stability of the $\text{Mg}_3(\text{BH}_4)_4(\text{NH}_2)_2$ compound.

References

- (1) Larcher, D; Tarascon J.-M. Towards Greener and More Sustainable Batteries for Electrical Energy Storage. *Nat. Chem.* **2015**, *7*, 19–29.
- (2) Anderson, D. L. *Theory of the Earth* **1998**.
- (3) Muldoon, J.; Bucur, C. B.; Gregory, T. Electrolyte Roadblocks to a Magnesium Rechargeable Battery. *Angew. Chemie Int. Ed.* **2017**, *56*, 12064–12084.
- (4) Deivanayagam, R.; Ingram, B. J.; Shahbazian-Yassar, R. Progress in Development of Electrolytes for Magnesium Batteries. *Energy Storage Mater.* **2019**, *21*, 136–153.
- (5) Zhao-Karger, Z.; Liu, R.; Dai, W.; Li, Z.; Diemant, T.; Vinayan, B. P.; Bonatto Minella, C.; Yu, X.; Manthiram, R.; Behm, R. J.; Ruben, M.; Fichtner, M. Toward Highly Reversible Magnesium–Sulfur Batteries with Efficient and Practical $\text{Mg}[\text{B}(\text{hfip})_4]_2$ Electrolyte. *ACS Energy Lett.* **2018**, *3*, 2005–2013.
- (6) Tutusaus, O.; Mohtadi, R.; Arthur, T. S.; Mizuno, F.; Nelson E. G.; Sevryugina, Y. V. An Efficient Halogen-Free Electrolyte for Use in Rechargeable Magnesium Batteries. *Angew. Chemie Int. Ed.* **2015**, *54*, 7900–7904.
- (7) Ding, M.S.; Diemant, T.; Behm, R. J.; Passerini, S.; Giffin, G. A. Dendrite Growth in Mg Metal Cells Containing $\text{Mg}(\text{TFSI})_2/\text{Glyme}$ Electrolytes. *J. Electrochem. Soc.* **2018**, *165*,

A1983-A1990.

- (8) Davidson, R.; Verma, A.; Santos, D.; Hao, F.; Fincher, C.; Xiang, S.; Van Buskirk, J.; Xie, K.; Pharr, M.; Mukherjee, P.; Banerjee, S. Formation of Magnesium Dendrites during Electrodeposition. *ACS Energy Lett.* **2019**, *4*, 375–376.
- (9) Jaschin, P. W.; Gao, Y.; Li, Y.; Bo S.-H. A Materials Perspective on Magnesium-Ion-Based Solid-State Electrolytes. *J. Mater. Chem. A* **2020**, *8*, 2875-2897.
- (10) Zhan, Y.; Zhang, W.; Lei, B.; Liu, H.; Li, W. Recent Development of Mg Ion Solid Electrolyte. *Front. Chem.* **2020**, *8*, 125.
- (11) Ikeda, S.; Takahashi, M.; Ishikawa, J.; Ito, K. Solid Electrolytes with Multivalent Cation Conduction. 1. Conducting Species in Mg-Zr-PO₄ System. *Solid State Ionics* **1987**, *23*, 125–129.
- (12) Yamanaka, T.; Hayashi, A.; Yamauchi, A.; Tatsumisago, M. Preparation of Magnesium Ion Conducting MgS-P₂S₅-MgI₂ Glasses by a Mechanochemical Technique. *Solid State Ionics* **2014**, *262*, 601–603.
- (13) Canepa, P.; Bo, S.-H.; Gautam, G. S.; Key, B.; Richards, W. D.; Shi, T.; Tian, Y.; Wang, Y.; Li, J.; Ceder, G. High Magnesium Mobility in Ternary Spinel Chalcogenides. *Nat. Commun.* **2017**, *8*, 1759.
- (14) Wang, L.; Zhao-Karger, Z.; Klein, F.; Chable, J.; Braun, T.; Schür, A.; Wang, C.; Guo, Y.; Fichtner, F. MgSc₂Se₄-A Magnesium Solid Ionic Conductor for All-Solid-State Mg Batteries? *Chem. Sus. Chem.* **2019**, *12*, 2286-2293.
- (15) Paskevicius, M.; Jepsen, L. H.; Schouwink, P.; Cerný, R.; Ravnsbæk, D.; Filinchuk, Y.; Dornheim, M.; Besenbacher, F.; Jensen T. R. Metal Borohydrides and Derivatives - Synthesis, Structure and Properties. *Chem. Soc. Rev.* **2017**, *46*, 1565-1634.
- (16) Roedern, E.; Kühnel, R.-S.; Remhof, A.; Battaglia, C. Magnesium Ethylenediamine Borohydride as Solid-State Electrolyte for Magnesium Batteries. *Sci. Rep.* **2017**, *7*, 46189.

- (17) Yan, Y.; Dononelli, W.; Jorgensen, M.; Grinderslev, J. B.; Lee, Y.-S.; Cho, Y. W.; Cerny, R.; Hammer, B.; Jensen, T. R. The Mechanism of Mg^{2+} Conduction in Amine Magnesium Borohydride Promoted by a Neutral Molecule. *Phys. Chem. Chem. Phys.*, DOI: 10.1039/d0cp00158a
- (18) Kisu, K.; Kim, S.; Inukai, M.; Oguchi, H.; Takagi, S.; Orimo, S. Magnesium Borohydride Ammonia-Borane as a Magnesium Ionic Conductor. *ACS Appl. Energy Mater.*, DOI: 10.1021/acsaem.0c00113
- (19) Jepsen, L. H.; Ley, M. B.; Lee, Y.; Cho, Y. W.; Dornheim, M.; Jensen, J. O.; Filinchuk, Y.; Jørgensen, J.; Besenbacher F.; Jensen, T. R. Boron–Nitrogen Based Hydrides and Reactive Composites for Hydrogen Storage. *Materials Today* **2014**, *17*, 129-135.
- (20) Higashi, S.; Miwa, K; Aoki, M.; Takechi, K. A Novel Inorganic Solid State Ion Conductor for Rechargeable Mg Batteries. *Chem. Commun.* **2014**, *50*, 1320–1322.
- (21) Le Ruyet, R.; Berthelot, R.; Salager, E.; Florian, P.; Fleutot, B.; Janot, R. Investigation of $Mg(BH_4)(NH_2)$ -Based Composite Materials with Enhanced Mg^{2+} Ionic Conductivity. *J. Phys. Chem. C* **2019**, *123*, 10756–10763.
- (22) Borgschulte, A.; Jones, M. O.; Callini, E.; Probst, B.; Kato, S.; Züttel, A.; David W. I.; Orimo, S. Surface and Bulk Reactions in Borohydrides and Amides. *Energy Environ. Sci.* **2012**, *5*, 6823.
- (23) Noritake, T.; Miwa, K.; Aoki, M.; Matsumoto, M.; Towata, S.; Li, H.-W.; Orimo, S. Synthesis and Crystal Structure Analysis of Complex Hydride $Mg(BH_4)(NH_2)$. *Int. J. Hydrogen Energy* **2013**, *38*, 6730–6735.
- (24) Jacobs, H. Die Kristallstruktur des Magnesiumamids. *Zeitschrift für Anorg. und Allg. Chemie* **1971**, *382*, 97–109.
- (25) Dimitrievska, M.; White, J. L.; Zhou, W.; Stavila, V.; Klebanoff, L. E.; Udovic, T. J. Structure-Dependent Vibrational Dynamics of $Mg(BH_4)_2$ Polymorphs Probed with Neutron

- Vibrational Spectroscopy and First-Principles Calculations. *Phys. Chem. Chem. Phys.* **2016**, *18*, 25546–25552.
- (26) Yang, Y.; Liu, Y.; Li, Y.; Gao, M.; Pan, H. Synthesis and Thermal Decomposition Behaviours of Magnesium Borohydride Ammoniates with Controllable Composition as Hydrogen Storage Materials. *Chem. Asian J.* **2013**, *8*, 476–481.
- (27) Jepsen, L. H.; Ban, V.; Møller, K. T.; Lee, Y.-S.; Cho, Y. W.; Besenbacher, F.; Filinchuk, Y.; Skibsted, J.; Jensen, T. R. Synthesis, Crystal Structure, Thermal Decomposition, and ^{11}B MAS NMR Characterization of $\text{Mg}(\text{BH}_4)_2(\text{NH}_3\text{BH}_3)_2$. *J. Phys. Chem. C* **2014**, *118*, 12141–12153.
- (28) Famprikis, T.; Canepa, P.; Dawson, J. A.; Islam, S.; Masquelier, C. Fundamentals of Inorganic Solid-State Electrolytes for Batteries. *Nature Mat.* **2019**, *18*, 1278-1291.
- (29) Adamu, M.; Kale, G. M. Novel Sol–Gel Synthesis of $\text{MgZr}_4\text{P}_6\text{O}_{24}$ Composite Solid Electrolyte and Newer Insight into the Mg^{2+} -Ion Conducting Properties using Impedance Spectroscopy. *J. Phys. Chem. C* **2016**, *120*, 17909–17915.
- (30) Imanaka, N.; Okazaki, Y.; Adachi, G. Divalent Magnesium Ionic Conduction in the Magnesium Phosphate-Based Composites. *Chem. Lett.* **1999**, *28*, 939–940.

TOC Graphic

